

amount of ASODNs delivered using antisense nanoparticles (0.024 nmol ASNP: 2.64 nmol ASODN); however, extreme toxicity was observed in both cases as measured by cell death, so we lowered the amount of ASODN and transfection reagent to the point that one strand of transfected ASODN was equivalent to one antisense particle (0.024 nmol ASNP: 0.024 nmol ASODN). In these cases, ASODNs transfected with either Lipofectamine or Cytofectin resulted in only ~6 to 8% knockdown in EGFP expression (Table 1). Evaluation of multiple cell lines (23) to determine toxicity limits of the ODN-Au NPs have not shown any appreciable cell death even with high (0.12 nmol) particle loadings.

Although these systems have not yet been optimized for maximum efficacy, the ability to systematically control the oligonucleotide loading on the NP surface has allowed us to identify several features that make them attractive candidates for antisense studies and therapies. The ability to modify the gold nanoparticle surface allows one to realize unusual cooperative properties that lead to enhanced target binding and allows the introduction of a variety of functional groups that have proven to be informative in terms of studying how the structure works within a cell. Moreover, this platform will allow us and others to add functionality (31, 32) that could direct the oligonucleotide-modified nanoparticle agents to specific cell

types and different components within the cell, thus opening the door for new possibilities in the study of gene function and nanotherapies.

#### References and Notes

- S. D. Patil, D. G. Rhodes, D. J. Burgess, *AAPS J.* **7**, E61 (2005).
- M. T. McManus, P. A. Sharp, *Nat. Rev. Genet.* **3**, 737 (2002).
- I. Lebedeva, C. A. Stein, *Annu. Rev. Pharmacol. Toxicol.* **41**, 403 (2001).
- T. L. H. Jason, J. Koropatrick, R. W. Berg, *Toxicol. Appl. Pharm.* **201**, 66 (2004).
- M. L. Stephenson, P. C. Zamecnik, *Proc. Natl. Acad. Sci. U.S.A.* **75**, 285 (1978).
- P. C. Zamecnik, M. L. Stephenson, *Proc. Natl. Acad. Sci. U.S.A.* **75**, 280 (1978).
- D. J. Bharali *et al.*, *Proc. Natl. Acad. Sci. U.S.A.* **102**, 11539 (2005).
- A. U. Bielinska, C. L. Chen, J. Johnson, J. R. Baker, *Bioconjugate Chem.* **10**, 843 (1999).
- M. Thomas, A. M. Klibanov, *Proc. Natl. Acad. Sci. U.S.A.* **100**, 9138 (2003).
- P. Sundaram, W. Xiao, J. L. Brandsma, *Nucleic Acids Res.* **24**, 1375 (1996).
- K. K. Sandhu, C. M. McIntosh, J. M. Simard, S. W. Smith, V. M. Rotello, *Bioconjugate Chem.* **13**, 3 (2002).
- M. M. Ow Sullivan, J. J. Green, T. M. Przybycien, *Gene Ther.* **10**, 1882 (2003).
- C.-P. Jen *et al.*, *Langmuir* **20**, 1369 (2004).
- C. A. Mirkin, R. L. Letsinger, R. C. Mucic, J. J. Storhoff, *Nature* **382**, 607 (1996).
- R. Jin, G. Wu, Z. Li, C. A. Mirkin, G. C. Schatz, *J. Am. Chem. Soc.* **125**, 1643 (2003).
- A. K. R. Lytton-Jean, C. A. Mirkin, *J. Am. Chem. Soc.* **127**, 12754 (2005).
- N. L. Rosi, C. A. Mirkin, *Chem. Rev.* **105**, 1547 (2005).
- R. Elghanian, J. J. Storhoff, R. C. Mucic, R. L. Letsinger, C. A. Mirkin, *Science* **277**, 1078 (1997).
- J.-M. Nam, C. S. Thaxton, C. A. Mirkin, *Science* **301**, 1884 (2003).
- L. He *et al.*, *J. Am. Chem. Soc.* **122**, 9071 (2000).
- D. J. Maxwell, J. R. Taylor, S. M. Nie, *J. Am. Chem. Soc.* **124**, 9606 (2002).
- J.-R. Bertrand, M. Pottier, A. Vekris, P. Opolon, A. Maksimenko, C. Malvy, *Biochem. Biophys. Res. Commun.* **296**, 1000 (2002).
- Materials and methods are available as supporting material on Science Online.
- A. G. Tkachenko *et al.*, *Bioconjugate Chem.* **15**, 482 (2004).
- E. Dulkeith, A. C. Morteau, T. Niedereichholz, T. A. Klar, J. Feldmann, *Phys. Review Letters* **89**, 20 203002-1 (2002).
- Han *et al.*, *Bioconjugate Chem.* **16**, 1356 (2005).
- Anderson *et al.*, *Chem.-Biol. Interact.* **112**, 1 (1998).
- R. L. Letsinger, R. Elghanian, G. Viswanadham, C. A. Mirkin, *Bioconjugate Chem.* **11**, 289 (2000).
- Z. Li, R. Jin, C. A. Mirkin, R. L. Letsinger, *Nucleic Acids Res.* **30**, 1558 (2002).
- Z. Wang, A. G. Kanaras, A. D. Bates, R. Cosstick, M. Brust, *J. Mater. Chem.* **14**, 578 (2004).
- J. M. Bergen, S. H. Pun, *MRS Bull.* **30**, 663 (2005).
- R. Weissleder, K. Kelly, E. Y. Sun, T. Shtatland, L. Josephson, *Nat. Biotechnol.* **23**, 1418 (2005).
- C.A.M. gratefully acknowledges a NIH Director's Pioneer Award and a National Cancer Institute—Center of Cancer Nanotechnology Excellence grant for support of this research. The authors thank T. O'Halloran, T. Meade, L. Shea, V. Band, H. Godwin, C. B. Gurumurthy, R. I. Morimoto, W. R. Russin, The Biological Imaging Facility, and the Keck Biophysics Facility for assistance.

#### Supporting Online Material

[www.sciencemag.org/cgi/content/full/312/5776/1027/DC1](http://www.sciencemag.org/cgi/content/full/312/5776/1027/DC1)

Materials and Methods

Figs. S1 to S4

30 January 2006; accepted 5 April 2006

10.1126/science.1125559

## Preparation of Poly(diiododiacetylene), an Ordered Conjugated Polymer of Carbon and Iodine

Aiwu Sun, Joseph W. Lauher, Nancy S. Goroff\*

Conjugated organic polymers generally must include large substituents for stability, either contained within or appended to the polymer chain. In polydiacetylenes, the substituents fulfill another important role: During topochemical polymerization, they control the spacing between the diyne monomers to produce an ordered polymer. By using a co-crystal scaffolding, we have prepared poly(diiododiacetylene), or PIDA, a nearly unadorned carbon chain substituted with only single-atom iodine side groups. The monomer, diiodobutadiyne, forms co-crystals with bis(nitrile) oxalamides, aligned by hydrogen bonds between oxalamide groups and weak Lewis acid-base interactions between nitriles and iodoalkynes. In co-crystals with one oxalamide host, the diyne undergoes spontaneous topochemical polymerization to form PIDA. The structure of the dark blue crystals, which look copper-colored under reflected light, has been confirmed by single-crystal x-ray diffraction, ultraviolet-visible absorption spectroscopy, and scanning electron microscopy.

Since Heeger, McDiarmid, and Shirakawa's discovery of conducting behavior in doped polyacetylene samples (1), carbon-rich molecules and materials have attracted great interest for their electronic and optical proper-

ties. Recently examined applications include photovoltaic cells, organic light-emitting diodes (OLEDs), field-effect transistors, and chemical sensors (2–5). Polyacetylene, the simplest conjugated polymer, consists of a backbone of carbon atoms, each bonded to one hydrogen atom and connected together by alternating single and double bonds. However, this material is thermally unstable and insoluble, making it unsuitable for general use. More manageable conjugated poly-

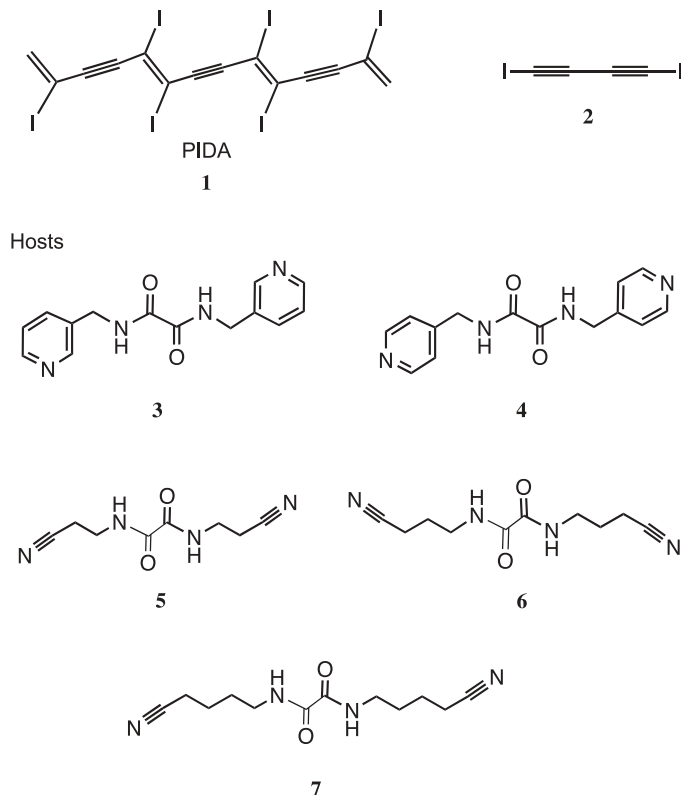
mers can be prepared from substituted alkynes (6) and other conjugated monomers, such as substituted aromatics; for example, in the commercially useful polymer poly(*p*-phenylenevinylene) (PPV), the backbone contains benzene rings as well as simple carbon-carbon double bonds. Polydiacetylenes, in which every other double bond in the polyacetylene backbone is replaced by a triple bond, are potent multiphoton absorbers that have applications in optical limiters, waveguides, and thermometric sensors (2).

Obtaining the desired optical and electronic properties of a given conjugated polymer requires a highly ordered molecular structure. For polydiacetylenes, this presents a substantial synthetic challenge: With solution-phase methods, the monomer diynes can react in either a 1,2- or 1,4-fashion, leading to a polymer with an irregular, branched backbone instead of regular repeat units. However, as discovered by Wegner (7) and elaborated by Baughman (8), if the diynes are first aligned appropriately in the solid state at a distance commensurate with the repeat distance in the target polymer, then their arrangement in space will control their reactivity, leading to ordered topochemical polymerization. Chemists have developed many creative approaches to induce appropriate alignment for 1,4-polymerization, not only in the solid state, but also in Langmuir-Blodgett films, liposomes and vesicles, and other ordered chemical interfaces (2, 9, 10). Hydrogen bonding has often

Department of Chemistry, State University of New York, Stony Brook, NY 11794-3400, USA.

\*To whom correspondence should be addressed. E-mail: nancy.goroff@sunysb.edu

**Fig. 1.** PIDA (**1**) and monomer **2**, shown with several Lewis-basic host molecules, including new compounds **5** to **7**.



played a key role in these methods; for example, with monomers that do not align properly on their own, hydrogen bonding to a partner compound can produce co-crystals that have the appropriate repeat distance for 1,4-polymerization (10, 11).

Nonetheless, the polydiacetylene structures accessible by these routes have been limited. For example, phenyl-substituted polydiacetylenes are desirable targets predicted to have particularly strong nonlinear optical absorptions, but there have been very few reported poly(aryldiacetylenes) (12, 13). Monomers such as diphenylbutadiyne do not align properly for 1,4-polymerization on their own and do not contain hydrogen-bonding functional groups to interact with an appropriate co-crystallizing agent.

Poly(diiododiacetylene), or PIDA (**1**, Fig. 1), represents a possible solution to the general problem of polydiacetylene synthesis. PIDA contains the polydiacetylene backbone but with only halogen-atom substituents. The abundance of transition metal-catalyzed reactions available for adding substituents in place of a carbon-halogen bond makes PIDA a potential precursor to a wide variety of polydiacetylenes.

Polymer **1** may also act as a precursor to carbyne, the hypothesized linear *sp*-hybridized allotrope of carbon ( $-C\equiv C-$ )<sub>n</sub>, which has thus far eluded definitive synthesis (14, 15). Researchers have approached carbyne by rational synthesis of discrete polyyne rods (values of *n* from 2 to 14), allowing for the prediction of

many of its properties (16–19). In addition, scientists have used electro- or thermochemical carbonization of small-molecule and polymeric substrates to make macroscopic carbyne-like materials consisting of polyyne domains and *sp*<sup>2</sup> hybridized kinks clustered around impurities in the samples. Hlavatý and co-workers have examined diiodobutadiyne (**2**), contained within the zeolite MCM-41, as a precursor to carbyne and found that ultraviolet irradiation could remove roughly half the iodine atoms of the starting material (20). However, producing a carbyne sample with a uniform structure that can be fully characterized remains a major challenge.

PIDA (**1**) is a promising precursor to fully ordered carbyne. With its linear arrangement of carbon atoms and small number of substituents, transformation of PIDA to carbyne requires only the cleaving of the carbon-iodine bonds and no further rearrangements. Electrochemical reduction of single-crystal PIDA samples would provide a previously unknown route to carbyne as an ordered material.

To prepare polymer **1** requires ordered alignment of the monomer diiodobutadiyne (**2**). Diiodobutadiyne was first reported by Baeyer in 1885 (21). It is moderately stable, decomposing rapidly and sometimes explosively when heated above its melting temperature of about 95°C (21–23). At room temperature, it can explode if subjected to physical shock, and it decomposes slowly under ambient light, forming an insoluble material with a graphite-like appearance (22). The decomposed material also explodes when heated, again releasing iodine gas (21). However, diiodobutadiyne can be handled safely at room temperature in gram quantities and decomposes very slowly if stored at –10°C in the dark. In solution, if exposed to light, it undergoes a very slow disproportionation reaction to give first tetraiodobutatriene and then hexaiodobutadiene, along with carbon-rich polymeric material (20, 24).

Although compound **2** has been known for over a century, efforts to determine its crystal structure precisely have been unsuccessful. As

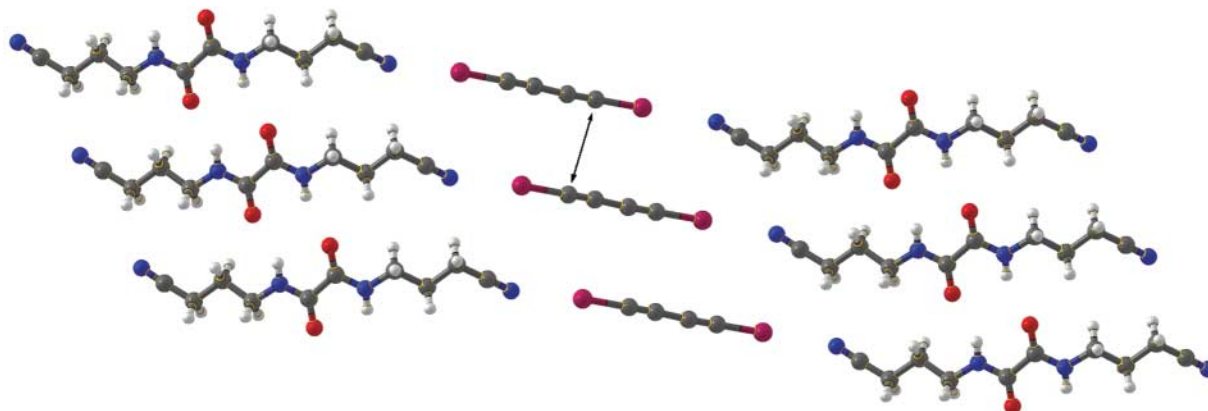


**Fig. 2.** Molecular packing in the co-crystal of **2** and **6**. The repeat distance is 5.25 Å, with a C1-C4' intermolecular contact distance (indicated by the arrow) of 4.0 Å and a declination angle of 51.3°.

a linear, rod-shaped molecule, diyne **2** forms needle-shaped crystals that are disordered along the direction of the molecular axis. In these crystals, the alignment between adjacent monomers is random, preventing ordered polymerization. Thus, the observed decomposition products formed from solid **2** do not have the structure of polymer **1** but instead are disordered materials of varying composition and connectivity.

To create ordered crystals of diyne **2** with controlled molecular spacing, we take advantage of another property of the monomer, namely the strong Lewis acidity of its iodine substituents (25–27). Iodine atoms in general are highly polarizable and therefore Lewis acidic. In iodoalkynes, this effect is magnified because *sp* hybridization increases the electronegativity of the carbon atom bonded to iodine, polarizing the C–I bond toward carbon. Gas-phase calculations and solution-phase experiments indicate that the interactions between iodoalkynes and individual Lewis bases are somewhat weaker than comparable hydrogen bonds (27–29). Even so, such interactions between Lewis-acidic iodines and appropriate bases are often called “halogen bonds,” in analogy to the more common hydrogen bond, and they have been demonstrated as a reliable organizational motif in the solid state (30–32).

Iodoalkyne halogen bonds have been used by Yamamoto, Kato, and co-workers, who have prepared multicomponent materials containing organic radical cation salts and neutral iodoalkynes (33, 34). In these systems, interactions between the Lewis-acidic iodoalkyne and the halide counter ion of the salt determine the spacing of the cations and therefore the electronic properties of the materials.

Alone, rod-shaped diiodobutadiyne forms crystals that are disordered along the long dimension of the molecule and therefore unsuitable for controlled topochemical polymerization. We previously demonstrated (32) that the Lewis acidity of the iodine atoms in **2** can be exploited to align the diyne in co-crystals with Lewis-basic hosts such as **3** and **4** (Fig. 1). However, efforts to polymerize **2** topochemically to form PIDA in these crystals have been unsuccessful, hampered by steric crowding around the iodines. To overcome these steric problems, we have now prepared a series of new host molecules, compounds **5** to **7** (35).

Like hosts **3** and **4**, compounds **5** to **7** each contain a central oxalamide group, designed to act as the primary organizing structure in the co-crystals. Fowler, Lauher, and co-workers have demonstrated that oxalamides form self-complementary hydrogen bonding networks with

a repeat distance (4.9 to 5.1 Å) that matches well the 4.9 Å distance requirement for diyne 1,4-polymerization (36, 37). In compounds **5** to **7**, linear alkyl nitrile chains replace the planar pyridyl groups of hosts **3** and **4**. We have prepared these new hosts from the corresponding aminoalkyl nitriles by condensation with diethyl oxalate. Although nitriles are weaker Lewis bases than pyridine nitrogen, previous experiments have indicated that they do act as electron donors to iodoalkynes in solution (27).

To form co-crystals of monomer **2** with each host, we prepared a 1:1 solution with 0.01 M concentration in methanol. Slow evaporation provided crystals for further analysis. From experiments with the three new hosts, we obtained three different results. Host **5** has much lower solubility than that of diyne **2**, and it precipitated from solution alone. However, both **6** and **7** formed co-crystals with **2**. In the case of host **6**, these co-crystals contained monomer **2**, as expected. In the case of host **7**, however, the isolated co-crystals contained PIDA, polymer **1**, which formed spontaneously under the crystallization conditions.

In the crystal structure of the **2**•**6** co-crystal (Fig. 2), much like the co-crystals of host **3** or **4** with **2**, the nitrile nitrogens are halogen-bonded to the iodines of **2**, but the repeat dis-

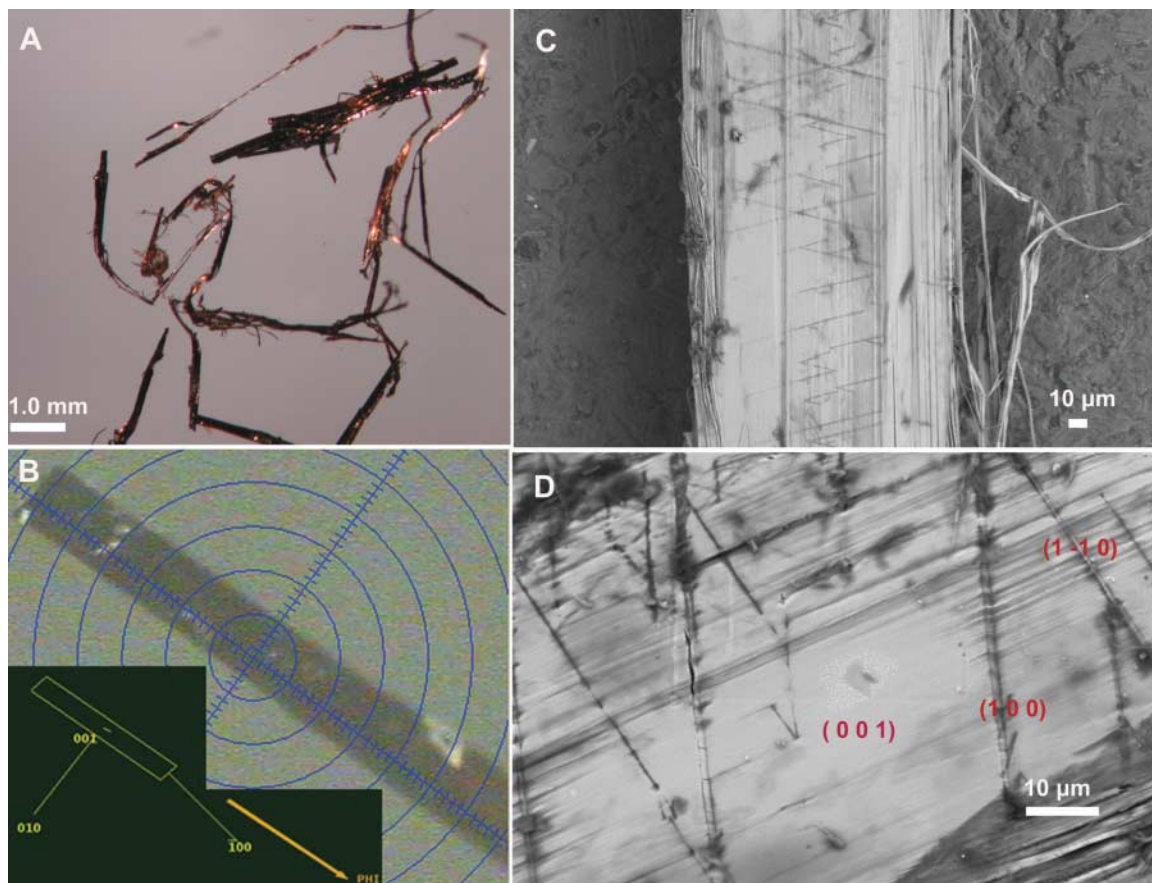


**Fig. 3.** Morphology of PIDA. (A) Microscopic image taken under polarized light with a Nikon SMZ800 optical microscope (Nikon Instruments, Incorporated, Melville, New York), (B) crystal faces identified by single-crystal x-ray diffraction analysis, and (C and D) field-emission SEM images of a crystalline PIDA fiber (FE-SEM LEO 1550, LEO Electron Microscopy, Thornwood, New York).

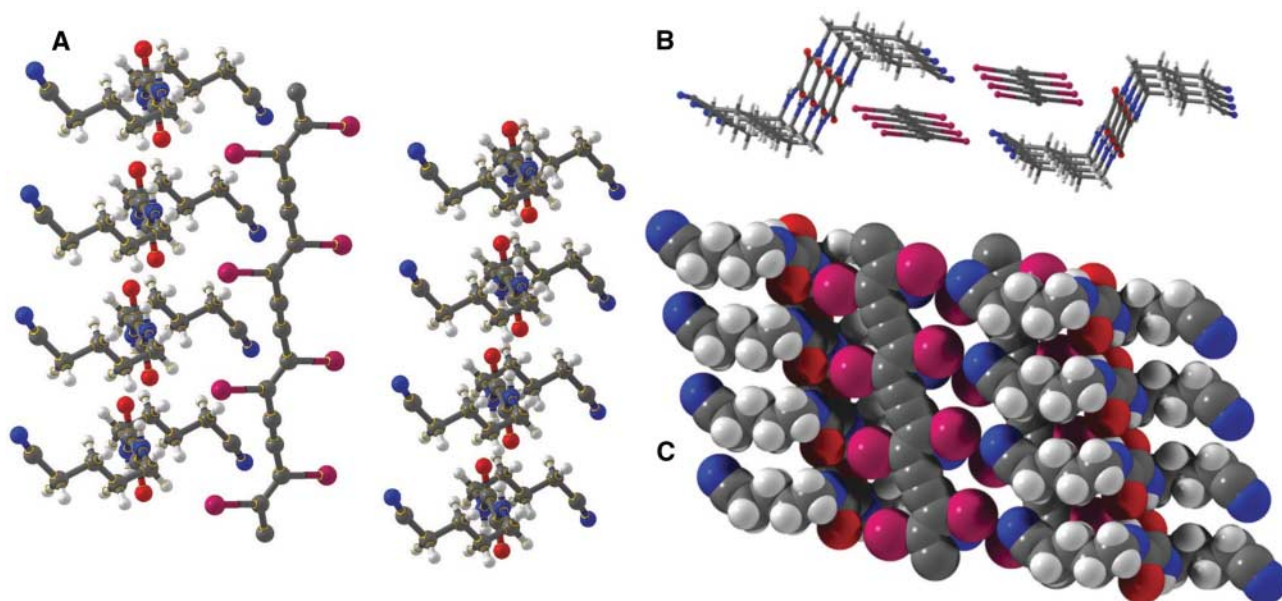


**Fig. 4.** Co-crystals of PIDA (**1**) and host **7**, as determined by x-ray diffraction (39). (A) A single polymer chain and hosts, (B) top view in ball-and-stick representation, and (C) side view in space-filling representation.

tance (5.25 Å) is longer than the targeted 4.9 Å needed for polymerization. Attempts to induce polymerization in these co-crystals have thus far been unsuccessful.

Whereas the **2**•**6** co-crystals are brown in color, the co-crystals isolated from solutions containing **2** and **7** are deep blue-purple; under reflected light, they have a coppery appearance and look like wire filaments (Fig. 3A). X-ray diffraction experiments established that these co-crystals contain polymer **1** rather than monomer **2** (Fig. 4). In the crystal structure, the polymer strands are all parallel to the oxalamide hydrogen-bonding network, with a repeat distance of 4.94 Å, close to the expected value of 4.9 Å. The host nitriles are each halogen-bonded to iodine atoms, as predicted. Unexpectedly, however, half the iodine atoms of **1** in the crystal have close contacts to oxalamide oxygen atoms rather than nitrile nitrogens, leading to a stoichiometry of 1:2 instead of the predicted 1:1 ratio. The oxygen atoms of host **7** are simultaneously acting as hydrogen-bond acceptors, suggesting that any stabilization from the oxygen-iodine interaction is likely quite small, although it contributes to the crystal packing structure.

We have been able to prepare co-crystals of **1** and **7** with lengths of up to 2 cm. Scanning electron microscopy (SEM) reveals the fibrous nature of these crystals, consistent with the alignment of the polymer strands within each crystal (Fig. 3, C and D). X-ray diffraction experiments confirm that the long dimension in these crystals corresponds to the (100) axis, the direction of polymer growth. In addition, the SEM images of the crystals include periodic linear steps, with heights of about 2 μm, either parallel to one another or crossing at an angle of 30°. X-ray diffraction experiments identify

these steps as corresponding to the (100) and (110) faces of the crystal, with the large flat surface corresponding to the (001) face.

By using host **7**, we have not obtained co-crystals containing unreacted monomer **2**. However, comparison with the **2**•**6** co-crystal structure indicates that the atoms of the guest likely undergo substantial motion upon polymerization (38). The flexibility of the host and the relative weakness of the interactions between host and guest may lower the barrier to such motion, making the polymerization reaction especially favorable.

At the same time, this flexibility and lack of directional preference may also be the source of some experimental difficulties. Although host **7** and monomer **2** reliably form polymer **1** in crystallite films from methanol solution, single crystals large enough for individual analysis, such as described above, can only be obtained haphazardly. Nonetheless, our studies of the crystallites indicated that they also contain polymer **1**. The electronic absorption spectra from these samples (fig. S1) exhibited a double-peak absorption with maxima at 594 nm (minor) and 650 nm (major), characteristic of an ordered polydiacetylene in the “blue phase,” where the polymer chains have fully planar, *s* trans conformation (2).

Although we have not yet measured the electrical conductivity of PIDA, the ability to obtain SEM images of the material at low voltages indicates qualitatively that polymer **1** is conducting. In addition, the SEM images highlight a benefit of topochemical synthesis. Because the polymer strands in the co-crystal are aligned, the electrical and optical properties of **1** will be highly anisotropic, with electronic and excitonic mobilities much higher along the (100) axis than in the other two di-

mensions. This anisotropy will allow for greater control in devices prepared from PIDA. At the same time, for solution-based applications, Lewis-basic solvents or co-solvents will interact with the iodine atoms of polymer **1**, increasing its solubility. The iodine atoms of **1** will therefore play a key role, not only in its synthesis, but also in future applications.

#### References and Notes

- H. Shirakawa, E. J. Louis, A. G. MacDiarmid, C. K. Chiang, A. J. Heeger, *J. Chem. Soc. Chem. Comm.* **1977**, 578 (1977).
- R. W. Carpick, D. Y. Sasaki, M. S. Marcus, M. A. Eriksson, A. R. Burns, *J. Phys. Cond. Matter* **16**, R679 (2004).
- J. M. Nunzi, *C. R. Phys.* **3**, 523 (2002).
- C. D. Dimitrakopoulos, P. R. L. Malenfant, *Adv. Mater.* **14**, 99 (2002).
- D. T. McQuade, A. E. Pullen, T. M. Swager, *Chem. Rev.* **100**, 2537 (2000).
- J. W. Y. Lam, B. Z. Tang, *Acc. Chem. Res.* **38**, 745 (2005).
- G. Wegner, *Z. Naturforsch. Teil B* **24**, 824 (1969).
- R. H. Baughman, *J. Polymer Sci. Polymer Phys. Ed.* **12**, 1511 (1974).
- D. Bloor, R. R. Chance, Eds., *Polydiacetylenes: Synthesis, Structure and Electronic Properties*, no. 102 of *NATO ASI Series E: Applied Sciences* (Nijhoff, Dordrecht, 1985).
- F. W. Fowler, J. W. Lauher, *J. Phys. Org. Chem.* **13**, 850 (2000).
- J. J. Kane, R. F. Liao, J. W. Lauher, F. W. Fowler, *J. Am. Chem. Soc.* **117**, 12003 (1995).
- A. Sarkar, S. Okada, H. Matsuzawa, H. Matsuda, H. Nakanishi, *J. Mater. Chem.* **10**, 819 (2000).
- Y. H. Chan, J. T. Lin, I. W. P. Chen, C. H. Chen, *J. Phys. Chem. B* **109**, 19161 (2005).
- L. Kavan, *Chem. Rev.* **97**, 3061 (1997).
- R. B. Heimann, S. E. Evsyukov, L. Kavan, *Carbyne and Carbynyoid Structures* (Kluwer Academic, Dordrecht, 1999).
- S. Hino, Y. Okada, K. Iwasaki, M. Kijima, H. Shirakawa, in *Nanonetwork Materials: Fullerenes, Nanotubes, and Related Systems*, vol. 590 of *AIP Conference Proceedings* (Springer, New York, 2001), pp. 521–524.
- T. Gibtner, F. Hampel, J.-P. Gisselbrecht, A. Hirsch, *Chem. Eur. J.* **8**, 408 (2002).
- S. Eisler et al., *J. Am. Chem. Soc.* **127**, 2666 (2005).
- Q. Zheng, J. A. Gladysz, *J. Am. Chem. Soc.* **127**, 10508 (2005).

20. J. Hlavatý, J. Rathousky, A. Zukal, L. Kavan, *Carbon* **39**, 53 (2000).
21. A. Baeyer, *Ber. Dtsch. Chem. Ges.* **18**, 2269 (1885).
22. F. Straus, L. Kollek, H. Hauptmann, *Ber. Dtsch. Chem. Ges. B* **63B**, 1886 (1930).
23. E. Heilbronner, V. Hornung, J. P. Maier, E. Kloster-Jensen, *J. Am. Chem. Soc.* **96**, 4252 (1974).
24. J. A. Webb, P.-H. Liu, O. L. Malkina, N. S. Goroff, *Angew. Chem. Int. Ed. Engl.* **41**, 3011 (2002).
25. C. Laurence, M. Queignec-Cabanetos, T. Dziembowska, R. Queignec, B. Wojtkowiak, *J. Am. Chem. Soc.* **103**, 2567 (1981).
26. C. Laurence, M. Queignec-Cabanetos, B. Wojtkowiak, *Can. J. Chem.* **61**, 135 (1983).
27. J. A. Webb, J. E. Klijn, P. A. Hill, J. L. Bennett, N. S. Goroff, *J. Org. Chem.* **69**, 660 (2004).
28. P. D. Rege, O. L. Malkina, N. S. Goroff, *J. Am. Chem. Soc.* **124**, 370 (2002).
29. W. N. Moss, N. S. Goroff, *J. Org. Chem.* **70**, 802 (2005).
30. P. Metrangolo, G. Resnati, *Chem. Eur. J.* **7**, 2511 (2001).
31. A. Cihfield *et al.*, *Cryst. Growth Des.* **3**, 313 (2003).
32. N. S. Goroff, S. M. Curtis, J. A. Webb, F. W. Fowler, J. W. Lauher, *Org. Lett.* **7**, 1891 (2005).
33. H. M. Yamamoto, J. I. Yamaura, R. Kato, *Synth. Met.* **102**, 1448 (1999).
34. H. M. Yamamoto, J. I. Yamaura, R. Kato, *Synth. Met.* **102**, 1515 (1999).
35. Materials and methods are available as supporting material on Science Online.
36. S. Coe *et al.*, *J. Am. Chem. Soc.* **119**, 86 (1997).
37. T. L. Nguyen, F. W. Fowler, J. W. Lauher, *J. Am. Chem. Soc.* **123**, 11057 (2001).
38. For example, in the **2•6** co-crystal, the iodine-nitrogen halogen bonding distance is 3.07 Å, and the C–I–N angle is 174.4°. In contrast, the iodine-nitrogen distance in the **1•7** co-crystal is 3.21 Å, and the C–I–N angle is 167.8°. The iodine-oxygen close contact is similar, with a distance of 3.20 Å and angle of 168.5°.
39. The unit cell parameters (triclinic,  $P\bar{1}$ ) are as follows :  $a = 4.944(2)$  Å,  $b = 9.142(3)$  Å,  $c = 15.051(5)$  Å,  $\alpha = 87.923(6)^\circ$ ,  $\beta = 84.590(6)^\circ$ ,  $\gamma = 78.759(7)^\circ$ ,  $V = 664.1(4)$  Å<sup>3</sup>,  $Z = 1$ .
40. We thank N. S. Sampson and H. Tang for their help in measuring the electronic absorption spectrum of PIDA. We are grateful to NSF (grants CHE-9984937, CHE-0446749, and CHE-0453334) for financial support of this research. Crystallographic details for the **1•7** and **2•6** co-crystals are available free of charge from the Cambridge Crystallographic Data Centre under deposition numbers CCDC 294370 and CCDC 294371, respectively.

#### Supporting Online Material

www.sciencemag.org/cgi/content/full/312/5776/1030/DC1

Materials and Methods

Figs. S1 to S3

Tables S1 and S2

5 January 2006; accepted 17 March 2006

10.1126/science.1124621

## Fast Mass Transport Through Sub-2-Nanometer Carbon Nanotubes

Jason K. Holt,<sup>1\*</sup> Hyung Gyu Park,<sup>1,2\*</sup> Yinmin Wang,<sup>1</sup> Michael Stadermann,<sup>1</sup> Alexander B. Artyukhin,<sup>1</sup> Costas P. Grigoropoulos,<sup>2</sup> Aleksandr Noy,<sup>1</sup> Olgica Bakajin<sup>1†</sup>

We report gas and water flow measurements through microfabricated membranes in which aligned carbon nanotubes with diameters of less than 2 nanometers serve as pores. The measured gas flow exceeds predictions of the Knudsen diffusion model by more than an order of magnitude. The measured water flow exceeds values calculated from continuum hydrodynamics models by more than three orders of magnitude and is comparable to flow rates extrapolated from molecular dynamics simulations. The gas and water permeabilities of these nanotube-based membranes are several orders of magnitude higher than those of commercial polycarbonate membranes, despite having pore sizes an order of magnitude smaller. These membranes enable fundamental studies of mass transport in confined environments, as well as more energy-efficient nanoscale filtration.

Carbon nanotubes, with diameters in the nanometer range and atomically smooth surfaces, offer a unique system for studying molecular transport and nanofluidics. Although the idea that water can occupy such confined hydrophobic channels is somewhat counter-intuitive, experimental evidence has confirmed that water can indeed occupy these channels (1, 2). Water transport through molecular-scale hydrophobic channels is also important because of the similarity of this system to transmembrane protein pores such as aquaporins (3). In recent years, numerous simulations (4, 5) of water transport through single-walled carbon nanotubes (SWNTs) have suggested not only that water occupies these channels, but also that fast molecular transport takes place, far in excess of what continuum hydrodynamic theories would predict if applied on this length scale. Molec-

ular dynamics (MD) simulations attribute this enhancement to the atomic smoothness of the nanotube surface and to molecular ordering phenomena that may occur on confined length scales in the 1- to 2-nm range (4, 5). For similar reasons, simulations of gas transport through SWNTs (6) predict flux enhancements of several orders of magnitude relative to other similarly sized nanoporous materials. Membrane-based gas separations, such as those using zeolites (7), provide precise separation and size exclusion, although often at the expense of

throughput or flux. It may be possible to use SWNTs to create a membrane that offers both high selectivity and high flux.

To investigate molecular transport on this length scale, we need to fabricate a carbon nanotube membrane that has a pore size of 1 to 2 nm. Researchers have recently fabricated multiwalled carbon nanotube (MWNT) membranes with larger pore diameters (6 to 7 nm) by encapsulation of vertically aligned arrays of MWNTs (8, 9) and by templated growth within nanochannel alumina (10). Enhanced water transport through these larger MWNTs has recently been reported (11). Quantifying transport through an individual tube in a MWNT membrane is difficult, however, because MWNTs are prone to blockages, in particular by “bamboo” structures and catalyst particles that can migrate to and obstruct the nanotube interior (9, 12, 13). The consequence of such blockages is a marked reduction of the active membrane pore density. In contrast, there are few, if any, reports of “bamboo” structure formation or catalyst migration for SWNTs or double-walled carbon nanotubes (DWNTs). However, it is difficult to produce vertically aligned carbon nanotubes of this size (14, 15). The major challenges also lie in finding a conformal deposition process to fill the gaps in this nanotube array, as well as in designing a selective etching process to open up the nanotube channels without producing voids in the membrane.

**Table 1.** Size exclusion tests on DWNT and MWNT membranes and molecular fluxes (per unit membrane area) of analytes. Values denoted by “<” were derived from the limits of detection for our concentration measurements when we did not observe any Au particles in the permeate solution. Differences of three to four orders of magnitude between this limiting value and the flux of the next smallest species indicate that the given analyte did not pass through the membrane.

| Analyte                              | Analyte size (nm) | DWNT membrane flux (molecules cm <sup>-2</sup> s <sup>-1</sup> ) | MWNT membrane flux (molecules cm <sup>-2</sup> s <sup>-1</sup> ) |
|--------------------------------------|-------------------|--|--|
| Ru <sup>2+</sup> (bipy) <sub>3</sub> | 1.3               | 5 × 10 <sup>13</sup>   | 5 × 10 <sup>13</sup>   |
| Colloidal Au 1                       | 2 ± 0.4           | <2 × 10 <sup>9</sup>   | 1 × 10 <sup>11</sup>   |
| Colloidal Au 2                       | 5 ± 0.75          | <3 × 10 <sup>8</sup>   | 3 × 10 <sup>10</sup>   |
| Colloidal Au 3                       | 10 ± 1            | Not tested   | <4 × 10 <sup>7</sup>   |

<sup>1</sup>Chemistry and Materials Science Directorate, Lawrence Livermore National Laboratory, Livermore, CA 94550, USA.

<sup>2</sup>Department of Mechanical Engineering, University of California, Berkeley, CA 94720, USA.

\*These authors contributed equally to this work.

†To whom correspondence should be addressed. E-mail: bakajin1@llnl.gov